Research Paper

Nifurtimox Inhibits the Progression of Neuroblastoma *in vivo*

Eryan Kong[1]✉*, Jiangli Zhu[2]*, Wentao Wu[3], Hongguang Ren[3], Xuemiao Jiao[1], Hui Wang [4,5]✉, Zhongjian Zhang[1]✉

1. Institute of Psychiatry and Neuroscience, Xinxiang Medical University, Xinxiang, China
2. Department of Ophthalmology, The Third Affiliated Hospital of Xinxiang Medical University, Xinxiang 453000, China
3. Tianjin Ocelean Pharma, Tianjin, China
4. Henan Key Laboratory of Immunology and Targeted Therapy, and
5. Henan Collaborative Innovation Center of Molecular Diagnosis and Laboratory Medicine, Xinxiang Medical University, Xinxiang, China;

*Equally contributed

✉ Corresponding authors: Institute of Psychiatry and Neuroscience, Xinxiang Medical University, Xinxiang, China. E-mail: 161066@xxmu.edu.cn; Handy: +86/17637323553

Abstract

Neuroblastoma was one of the most life-threatening cancer developed in children, yet the conventional therapies currently used leave an unmet gap for clinical requirements. Temozolomide is the first line of drug in the treatment of neuroblastorma nowadays. Giving the fact that temozolomide treatment offered limited healing effect and patients responded divergently, an alternative beneficial path is urgently requested. Nifurtimox, a drug against *Trypanosoma cruzi*, was happened to find competent in treating a patient who carried aggressive neuroblastoma. Although *in vitro* studies demonstrated that nifurtimox has cytotoxic features against tumor cells, a systematic investigation *in vivo* is generally inadequate. Here we exhibited that nifurtimox could suppress the progression of neuroblastoma *in vivo*, while maintain the health condition to a great extent. Importantly, as comparing to temozolomide, nifurtimox presented a stronger effect on inhibiting tumor development, strongly suggesting that nifurtimox is a preferential alternative drug in treating neuroblastoma. Additionally, it was shown that Akt-GSK3β signaling cascade was involved in tumor arrest induced by nifurtimox.

Key words: Neuroblastoma, Nifurtimox, Temozolomide, tumor suppression

Introduction

Neuroblastoma is one of the most common neonatal cancer and nearly half of the patients occurred were younger than 2 years old [1-3]. It originates from the sympathetic nervous system during embryonic development, which has a heterogeneous genetic background and substantial histological diversity, leading to differential presentation and behavior of tumor formation [3-6]. Hence, the treatment for neuroblastoma might have poor outcomes, often resulting in chemo-/radio-therapy resistance [7, 8]. The 5-year survival rate for patients with aggressive neuroblastoma was very low, varies from 10% to 30% [9, 10]. Current radio-and chemo-therapies for children was associated with severe toxicity and yielded only a few successful cases, hence, novel approaches are sorely demanded for the patients carrying these diseases.

Nifurtimox, a primary therapeutic drug against *Trypanosoma cruzi*, was found effective in treating an aggressive neuroblastoma patient who happened to be infected by *Trypanosoma cruzi* from a blood transfusion during her treatment [11-18]. A few studies *in vitro* presented that nifurtimox has cytotoxic features against tumor cells by inducing the formation of reactive oxygen species (ROS) under hypoxic conditions and thus triggers the apoptotic signaling pathways [8, 15, 19, 20]. Yet, systematic studies to show how nifurtimox hinders the progression of neuroblastoma *in vivo* were not sufficient. Plus,

comparing the anti-tumor efficacy of nifurtimox with that of a commonly prescribed neuroblastoma treatment drug should be valued. Aim of the present study was to first, investigate the efficacy and progression of Nifurtimox treatment against neuroblastoma *in vivo* analytically and then compare with that of a therapeutic drug i.e. temozolomide, commonly used against various types of neural tumors in clinic.

Materials and Methods

The construction of SY5Y cell line stably expressing firefly luciferase (luc2)

SY5Y cells were infected by lentivirus with pCDH-luc2-GFP plasmid. After 24 h, the cell culture medium was changed with fresh RPMI-1640 medium (Gibco, USA) containing 10% (v/v) super fine fetal bovine serum (Beijing Hengsheng Ma Yuan institute of biotechnology, batch no. 150913), coupled with puromycine for positive selection (Final concentration 1 ug/ml, Invivogene, USA). GFP signal was observed under fluorescence microscope after 7 days of culture, and the cell bioluminescence was measured by PekinElmer IVIS Spectrum CT imaging system.

Cell culture

Cell lines were maintained in RPMI-1640 medium (Gibco, USA) supplemented with 10% (v/v) superfine fetal bovine serum (Beijing Hengsheng Ma Yuan institute of biotechnology, batch no. 150913), 1% penicillin/streptomycin (Institute of engineering, Chinese academy of medical sciences, batch no. 20161015-0116,10000 IU/ml) at 37°C in a humidified incubator with 5% CO_2. The culture medium was changed every 1-2 d. For subculture, cells were treated with 0.25% trypsin for disassociation (Institute of biomedical engineering, Chinese academy of medical sciences. batch no. #TE2004Y) and centrifugated at 1000 r/min for 5 min, the supernatant was discarded and then re-suspended in the fresh culture medium.

Phospho-kinase array and Western blot

The Human Phospho-kinase array kit was purchased from R&D, catalog No: ARY003B. SH-SY5Y cells were cultured and prepared according to the procedures suggested by the instructions provided in the kit. Briefly, treated cells were harvested and equal amount of proteins were incubated with 1st and 2rd antibodies, which were then blotted for histochemical signals. The corresponding spot in blot was quantified by its grey value and statistically analyzed. Western blot was performed according to standard protocol, corresponding antibodies were used for detecting the signal: GSK-3β (cell signaling #12456), phosphor-GSK-3β (cell signaling #5558), AKT (cell signaling #4685), phosphor-AKT (cell signaling #4060) and HRP-anti-rabbit antibody.

Animals and Housing

8 week-old female Nu/Nu mice, weighted 18-20g, were purchased from Beijing Vital River Laboratory Animal Technology Co., Ltd., a distributor of Charles River Laboratories in China. Mice were housed in standard transparent laboratory cages in a temperature-controlled colony room (22 ± 1°C) and were provided with food and water ad libitum unless stated otherwise. Mice were maintained on a 12 hours light/dark cycle (with lights on at 6:00 am, 200-220 lux inside the cages). All experiments were designed to reduce animal suffering and keep the number of animals used at the minimum level. All animal procedures were performed according to guidelines approved by the committee on animal care at Xinxiang Medical University. The body weight and food intake were recorded on weekly basis.

Subcutaneous transplantation of human neuroblastoma

Prior to implantation, harvested the SH-SY5Y-luc2-GFP cells in the stage of logarithmic growth, briefly washed with PBS (Gibco, batch no. 8117080) and re-suspended in PBS at the concentration of 1×10^7 cells/ml. Nude mice was injected subcutaneously with the volume of 0.2 ml suspension cells, namely 2×10^6 cells.

The establishment of renal tumor disease model

When the subcutaneous transplanted tumor (SH-SY5Y-luc2-GFP) grew up to about 1-2 cm in diameter, the tumor block was removed under sterile condition, and was divided into tumor blocks in 1.0 mm^3. The nude mice were anesthetized and fixed on the operating table, then disinfected with betadine and 70% alcohol. The right kidney was exposed by opening from the back of the right side, then an incision about 1 cm long was introduced for the insertion of the tumor block with the casing needle. Sterile gauze was used to stop the bleeding and the handled kidney was returned after the operation, muscles and skins were then successively sutured.

Detecting the bioluminescence of renal tumor in living mice

The IVIS Spectrum CT imaging system was used to detect bioluminescence at various time points. First, mice were anesthesized with 2% isoflurane for preparation. Then, transfer the nude mice into the chamber of IVIS Spectrum CT machine while

maintaining the mice with isofluran (0.5%) for sleeping. Bioluminescence images were taken and last, quantify the detection signal with the imaging software coupled with the IVIS Spectrum CT system.

Design for the treated groups and drug administration experiment

After 7 days of Surgical implantation, the tumor bearing mice were re-imaged with IVIS Spectrum CT machine and every 10 mice was randomly assigned into different groups, which includes control, nifurtimox treated groups at the concentration of 50 mg/kg, 100 mg/kg, 200 mg/kg and the positive control group (temozolomide 30 mg/kg). Then the drugs were administered by gavage for 1 time/day at the dosage of 0.2ml /20g. All animals were daily checked for health condition and weighed every another day. The bioluminescence signal for the tumor progression was planned for every 5 days according to the health condition of the individual mice. All treated animals were sacrificed after treatment, kidney and tumor block were dissected, weighed and photographed. The tumor blocks were stored in 4% formaldehyde solution for potential pathological examination.

Statistical analysis

Basic descriptive data are presented as means standard deviations or standard errors. The rate of tumor growth = (The difference of luminescence intensity between the control group and the medicated group)/the luminescence intensity of the control group x 100%. Statistical analyses and graphs were created using GraphPad Prism software for Windows, version 5. The statistical analysis of each group was made via One-way ANOVA and two groups of Tukey's test, and the statistical analysis of each group at various time points was made via two-way ANOVA and the Bonferroni's test of the two groups.

Results

The progression of neuroblastoma is inhibited by Nifurtimox *in vivo*

To set up the *in vivo* xenograft disease model for imaging, the stable neuroblastoma cell line SH-SY5Y-luc2-GFP was generated by infection the human origin SH-SY5Y cells with lentivirus containing pCDH-luc2-GFP plasmid. SH-SY5Y-luc2-GFP cells was initially planted under the skin in nude mice (*nu/nu*) and taken out until tumor size reached 1-2 cm in diameter. The tumor tissue was sheared into 1.0 X 1.0 X 1.0 mm^3 for kidney transplantation, the expressed fluorescence signal was used for *in vivo* imaging by IVIS Spectrum CT. By taking the advantage of the imaging, we could visualize that the transplantation of SH-SY5Y-luc2-GFP cells into the right kidney was successful after 7 days of operation, all handled mice were in good condition (Fig.1A). Nifurtimox was tested for 3 different concentrations, 50mg/kg, 100mg/kg and 200mg/kg, according to a previous study showing that the dosage of nifurtimox at around 150mg/kg is well tolerated in mice [19]. For better evaluating the tumor-suppression efficacy, temozolomide, a usually prescribed anti-neural tumor drug in clinic, was included in the experiments at the dosage of 30mg/kg. Control group was exposed to the same concentration of DMSO used for dissolving the drugs. The treatment lasted for 9 days and all the mice were daily checked and weighted every another day. No mouse was lost during the experiment.

To visualize the progression of tumor development, the experimental mice were scanned 3 times during experiment i.e. 1-, 5-and 9-day(s) after initiating the drug treatment (Fig. 1A). By quantifying the tumor-fluorescence intensity, we could demonstrate that the neuroblastoma disease model is well established since the signal intensity for control group increased exponentially, as shown in Fig. 1A and 1B. More importantly, it was shown that after 5 days of treatment, there was already a significant difference (p≤0.05) in tumor-fluorescence intensity as comparing the nifurtimox-treated group (100mg/kg) with that of the control group, while the temozolomide-treated group did not present a similar result (Fig. 1B, middle panel). If the dosage of nifurtimox goes to the highest (200mg/kg), the nifrutimox-treated group demonstrated a very significant difference (p≤0.01) in tumor-fluorescence intensity as compared with that of the control group. Not surprisingly, when comparing the nifurtimox-treated group (200mg/kg) with the temozolomide-treated group, there was also a significant difference (p≤0.05) in tumor-fluorescence intensity (Fig. 1B, middle panel). After 9 days of treatment, the temozolomide-treated group showed a significant difference with that of the control group (Fig. 1B, right panel), verifying that temozolomide treatment was effective (magnified representative images shown in Fig. 2A and 2B,). While the nifurtimox-treated groups exhibited a stronger effect: at the concentration of 50mg/kg and 100mg/kg, the treatments displayed a very significant difference in hampering tumor growth with that of the control group (p≤0.01) and the treatment effect was even stronger for nifrutimox at the maximum concentration (200mg/kg, p≤0.001, Fig. 1B, right panel), also shown by the magnified representative images in Fig. 2C, 2D and 2E.
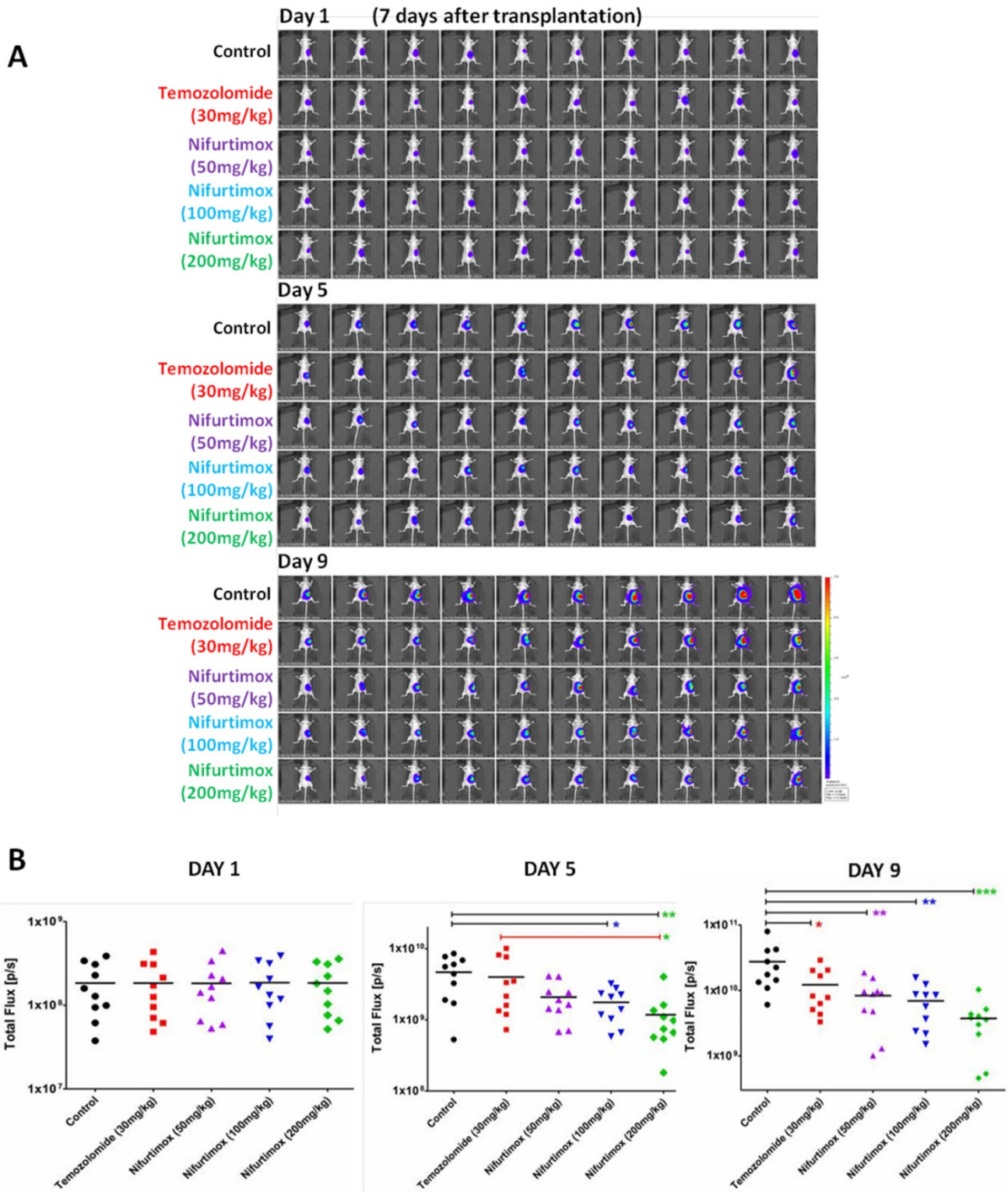
Figure 1. The progression of neuroblastoma is inhibited by Nifurtimox in vivo. A) The expressed *in vivo* fluorescent signal of SH-SY5Y-luc2-GFP was scanned by IVIS Spectrum CT. The first scan was done after 7 days of tumor cell transplantation and then initiated the drug treatment (Day 1), and two consecutive scans (Day 5 and Day9) were carried out every another 4 days for time series tracking. Different dosage of Temozolomide and Nifurtimox were used for drug treatment groups, control group was treated with the same concentration of DMSO used for dissolving drugs. B) The intensity of the fluorescent signal of SH-SY5Y-luc2-GFP was quantified and compared between different groups. * p≤0.05, ** p≤0.01, *** p≤0.001.

Above all, the data here presented that both nifurtimox and temozolomide inhibited the tumor growth effectively, when comparing the two type of treatments, nifurtimox appeared to take on effect in a much earlier and stronger manner than temozolomide.
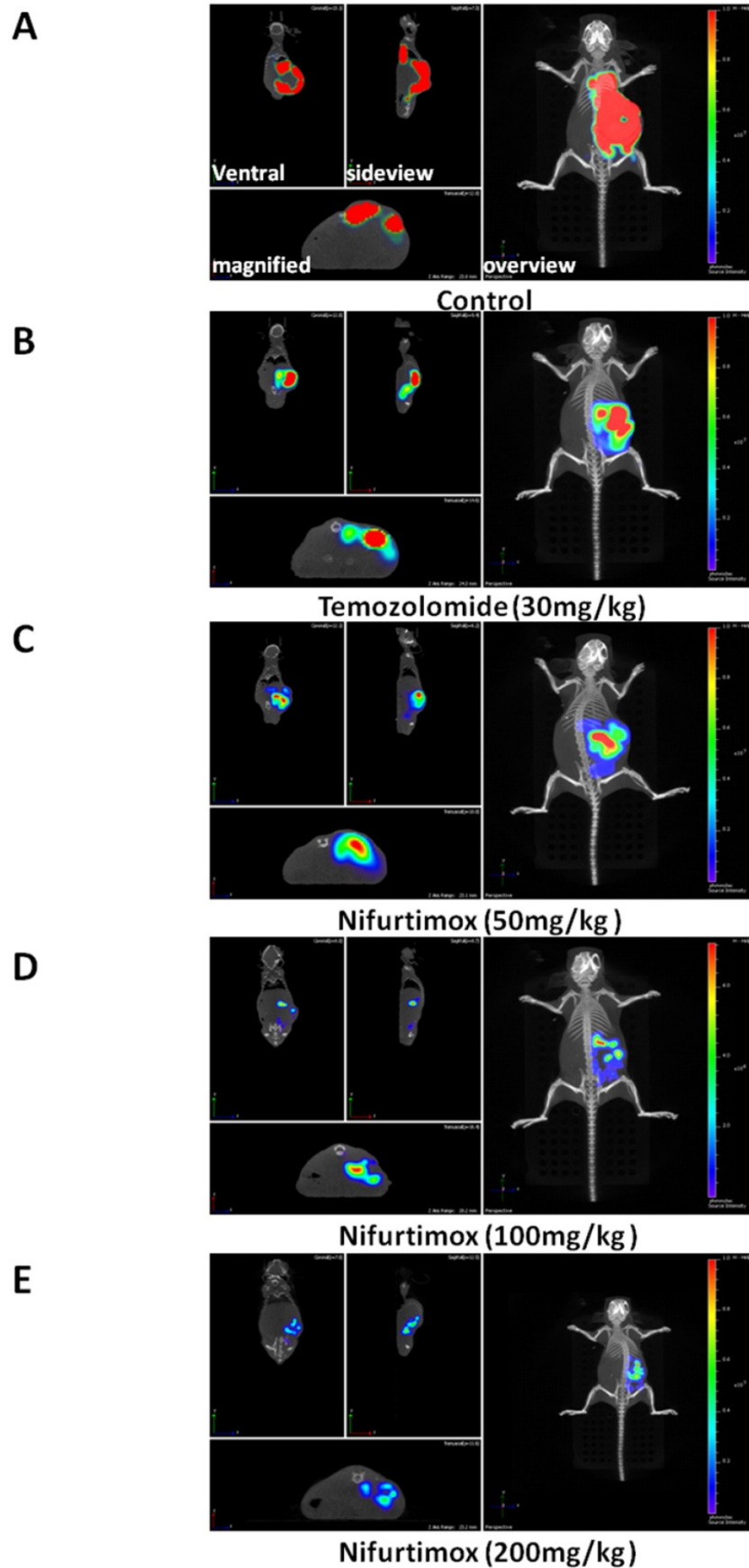
Figure 2. Nifurtimox was effective in treating neuroblastoma. A, B, C, D, E) representative images of treated mouse (Control and treated groups) were scanned either from overview or side-view, the fluorescence signal of tumor cells in situ was magnified and illustrated for comparison.

Nifurtimox impeded the neuroblastoma deterioration in situ

To analytically measure the tumor deterioration in vivo, all the treated mice were sacrificed after 9 days of treatment. Both kidneys were dissected out for imaging and weighted to assess the treatment effect. As shown in Fig. 3A, the size of the right kidney in the control group increased drastically as compared to that of the WT, suggesting that the neuroblastoma disease model was well established. The drug treatment groups using Temozolomide and nifurtimox manifested an inhibitory effect against tumor development since the size of the right kidney developed much smaller than that of control group (Fig. 3A). The quantification results showed that the temozolomide treatment significantly hindered the tumor expansion ($p \leq 0.05$) and interestingly, all the nifurtimox-treated groups (50mg/kg, 100mg/kg and 200mg/kg) presented a very significant effect on tumor suppression than that of the control group ($p \leq 0.001$, Fig. 3B). Given the nifurtimox at the concentration of 200mg/kg, it manifested a mega robust effect on tumor arrest than that of the temozolomide-treated group (Fig.3B). To avoid the bias that the kidney weight varies individually, we normalized all the data by calculating the index of right kidney/body weight, the result obtained was consistent (Fig. 3C). All nifurtimox-treated groups (3 different concentrations) presented a stronger effect on tumor inhibition over the control group; similarly, the nifurtimox-treated group with 200mg/kg is pronounced in blocking tumor growth than that of the temozolomide-treated group (Fig. 3C). The weight of the left kidney remained unchanged for all groups, treated and untreated (Fig. 3D).

The results here demonstrated that the fierce extension of neuroblastoma could be blocked by nifurtimox and temozolomide in situ, while the former pill showed a better control of the tumor growth over the latter.

Body weight and tumor suppression efficacy were well balanced by nifurtimox

During the expansion of neuroblastoma or other types of tumors, the body constitution is usually deteriorated, indicating by the loss of body weight. Investigating to what extent the treatment affect the body condition, all mice were checked daily and weighted every another day. The quantification data acquired from the absolute body weight illustrated that the concentration of nifurtimox positively regulated the body weight in a dose-dependent manner i.e. after treatment, higher dosage of nifurtimox (200mg/kg) presented a better body condition than that of the lower dosage

nifurtimox-treated groups (50mg/kg and 100mg/kg) and the control group, while the temozolomide-treated group could not slow down the decrease of the body weight as compared to control (Fig. 4A). To assess the ability of withholding the decline of body weight between temozolomide- and nifurtimox-treated groups, it was not difficult to find out that nifurtimox treatment presented a much better effect than that of the temozolomide treatment (Fig. 4A).

To avoid of the bias that the body weight varies individually, the relative body weight was introduced, the body weight of day 1 was considered as 100% for each group and the data collected during treatment was normalized with that of day 1 accordingly. The obtained quantification analysis showed up a similar results as that of in the analysis of the absolute body weight i.e. the treatment using the highest concentration of nifurtimox (200mg/kg) exhibited the most strong effect on holding body weight than that of the low levels of nifurtimox, as well as the control group and temozolomide-treated group (Fig. 4B).

To compare the tumor suppression efficacy between nifurtimox and temozolomide, the value of the tumor-fluorescence intensity from spectrum CT (Fig. 1A and 1B) or the kidney weight (Fig. 3A, 3B and 3C) was used according to the following calculation formula: tumor suppression efficacy = 1 - (average value from treated group/average value from control group). The quantification data, either based on tumor-fluorescence intensity or the kidney weight displayed a very similar pattern, that in general, nifurtimox-treated group presented a higher tumor suppression efficacy than the temozolomide-treated group (Fig. 5A and 5C). Very interestingly, to correlate the tumor suppression efficacy with the according concentration of nifurtimox, we found out that these 2 factors correlate with each other in a nearly perfect linear relationship ($R^2 = 0.9994$ or $R^2 = 1$, Fig. 5B and 5D), proving that nifurtimox hinder the tumor growth in a dose dependent manner.

Two paired factors are always considered when evaluating a treatment drug i.e. tumor suppression efficacy and the ability to sustain the body weight. Our data presented above showed that nifurtimox balanced these two factors in a good manner, strongly suggesting that nifurtimox should have a huge potential for neuroblastoma treatment.

AKT-GSK3β signaling might be involved in the tumor-suppression induced by nifurtimox

Previous study demonstrated that nifurtimox inhibited tumor growth by suppressing the Akt phosphorylation and the cytotoxicity of nifurtimox

could be attenuated by a tyrosine hydroxylase inhibitor [19]. Considering the fact that Akt plays a central role in regulating various downstream signaling, we sought out to explore the potential downstream signaling regulated by Akt. The phospho-kinase array was applied for screening the Akt signaling pathways. The obtained results showed that the phosphorylation of GSK3β was up-regulated upon nifurtimox treatment as compared with DMSO-treated control group in SH-SY5Y cells, while other downstream effectors were found unaltered (Fig. 6A-C). These results suggested that nifurtimox inhibited Akt phosphorylation and furthermore triggered the up-regulation of GSK-3 β phosphorylation, therefore affected tumor growth which was well illustrated in current study (Fig. 1 and Fig. 3).
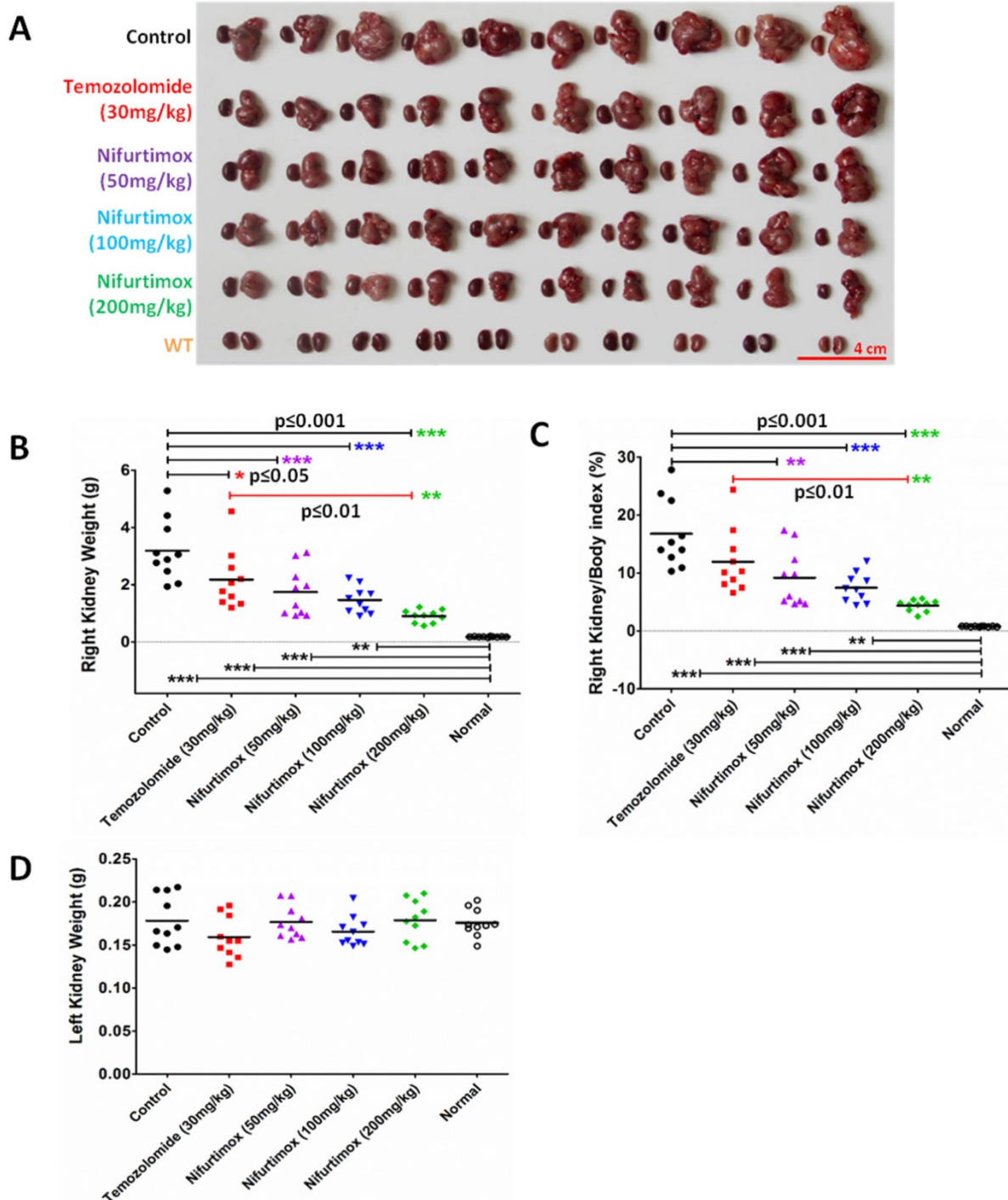

Figure 3. Nifurtimox impeded the expansion of neuroblastoma in situ. A) both kidneys were dissected out for direct evaluation of tumor progression. B, C, D) absolute or relative kidney weight was quantified between different treating groups for comparison. Nifurtimox was used for different concentration (50, 100 and 200 mg/kg), Temozolomide (30mg/kg) was used as positive control while DMSO treated group was used as control. * p≤0.05, ** p≤0.01, *** p≤0.001.
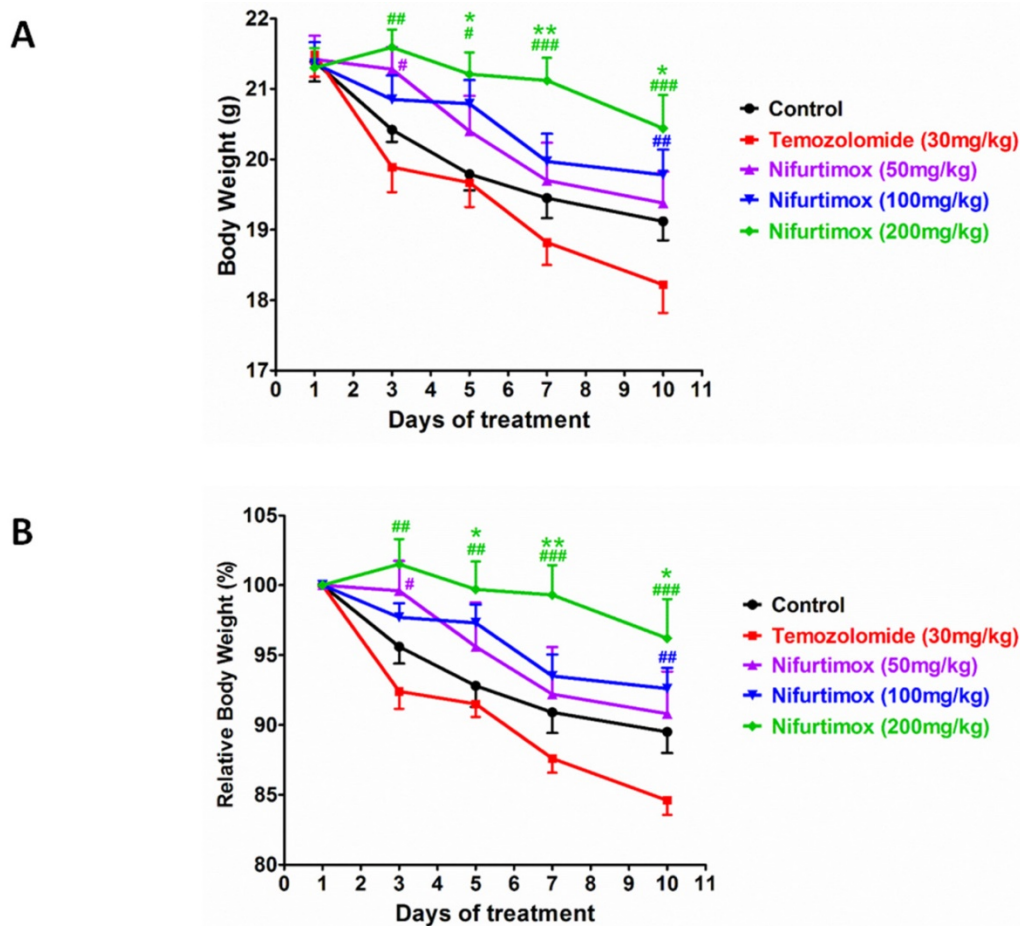
Figure 4. The body constitution is well maintained for Nifurtimox treatment. A and B) The absolute or relative body weight of mice were measured daily and plotted together for comparison. Nifurtimox was used for different concentration (50, 100 and 200 mg/kg), temozolomide (30mg/kg) was used as positive control while DMSO treated group was used as control. * p≤0.05 and ** p≤0.01 was labeled as compared with Control group, # p≤0.05, ## p≤0.01, ### p≤0.001 was labeled as compared with Temozolomide-treated group.

To figure out the mechanism generosity of nifurtimox in other cell types, i.e. whether nifurtimox would trigger the down-regulation of Akt signaling. Several tumor cell lines (H1299, U251 and N2a) were used, nifurtimox-treated cells showed a decreased level of phospho-Akt, and an increased level of phosphor-GSK-3β, as compared with that of the control group (Fig. 6E), which is in line with the findings in SH-SY5Y cells. Together, these results suggested that the deactivation of Akt-GSK-3β signaling might be a common mechanism for nifurtimox to hinder tumor growth.

Discussion

An initial point for selecting drugs treating cancer is that the drug compound should be able to suppress the proliferation or growth of tumor efficiently in vitro, which was well evaluated by previous studies for both temozolomide and nifurtimox [15-17, 21-25]. Temozolomide has anti-tumor activity against a variety of malignancies including glioma, metastatic melanoma and other

difficult-to-treat cancers [26-28]. Interestingly, nifurtimox also presented a broad spectrum of tumor-inhibition activity e.g. clonogenic tumor cells and neuroblastoma [8, 15-17, 19]. Disregard of their unalike molecular mechanism in inhibiting tumor growth [8, 19, 29, 30], here we systematically analyzed and compared their features in curbing the tumor progression *in vivo* as well as examining their physiological toxicity upon the dosage applied.

Data here presented that both nifurtimox and temozolomide could suppress the tumor growth significantly after 9 days of treatment *in vivo*, while nifurtimox displayed a better treatment effect over temozolomide (Fig. 1A and 1B, Fig. 2A-2E). Importantly, the tumor suppression efficacy of nifurtimox is linearly correlated with its concentration (Fig. 5A-5D), indicating that nifurtimox has a great potential in treating neural tumors. In addition, nifurtimox inhibited tumor growth in a more timely manner: after 5 days of treatment, nifurtimox (100 mg/kg and 200 mg/kg) hindered the tumor expansion significantly, yet temozolomide did not show the similar effect (Fig. 1B). In line with these

observations, when examining the anti-tumor ability of treatments from the perspective of measuring the weight of the right kidney, the experimental results illustrated that both nifurtimox and temozolomide could arrest the tumor development significantly after 9 days of treatment (Fig. 3A-3C). Critically, nifurtimox (200 mg/kg) manifested a stronger effect in restraining tumor increase as compared with that of temozolomide (Fig. 3B and 3C).

By knowing that nifurtimox could inhibit the growth of neuroblastoma in a time- and concentration-dependent manner, it is also critical to understand if nifurtimox treatment introduced severe toxicity when treating patients. One of the most important parameter to determine the rate of tissue toxicity was judging the loss of body weight, as illustrated by many clinical observations [31-33]. Excitingly, our data displayed that the higher concentration of nifurtimox showed a better capability of withholding body weight as compared to that of the lower concentrations of nifurtimox-treatments (Fig. 4A and 4B), while in general, nifurtimox treatments presented a stronger ability in keeping body weight than that of temozolomide (Fig. 4A and 4B), suggesting that nifurtimox could sufficiently suppress the tumor

progression and meaningfully decrease the deterioration of body health caused by tumor expansion and aggression. Such efficient tumor-suppression rate could be due to the fact that neuroblastoma contains catecholamines, which in turn enhance the cytotoxic effects of nifurtimox for neuroblatoma [19, 34].

The Akt-GSK3β signaling cascade plays critical roles in controlling cell cycle and tumor growth[35, 36]. Previous study demonstrated that nifurtimox could suppress the Akt signaling in neuroblastoma [19], which is line with our findings (N2a, Fig. 6E). Additionally, we showed that nifurtimox could suppress the activation of Akt-GSK-3β in other tumor types e.g. Lung cancer (H1299) and astroglioma (U251, Fig. 6E), indicating that prohibiting the Akt phosphorylation might be a general mechanism for nifurtimox to exert its function on tumor growth. Logically, as Akt phosphorylation is downregulated, the phosphorylation of GSK-3β shall be upregulated (Fig. 6D), which is truly supported by the results found in a phospho-kinase array (Fig. 6A-C). These findings pointed out that nifurtimox blocks tumor growth possibly by manipulating the signaling cascade of Akt-GSK3β.
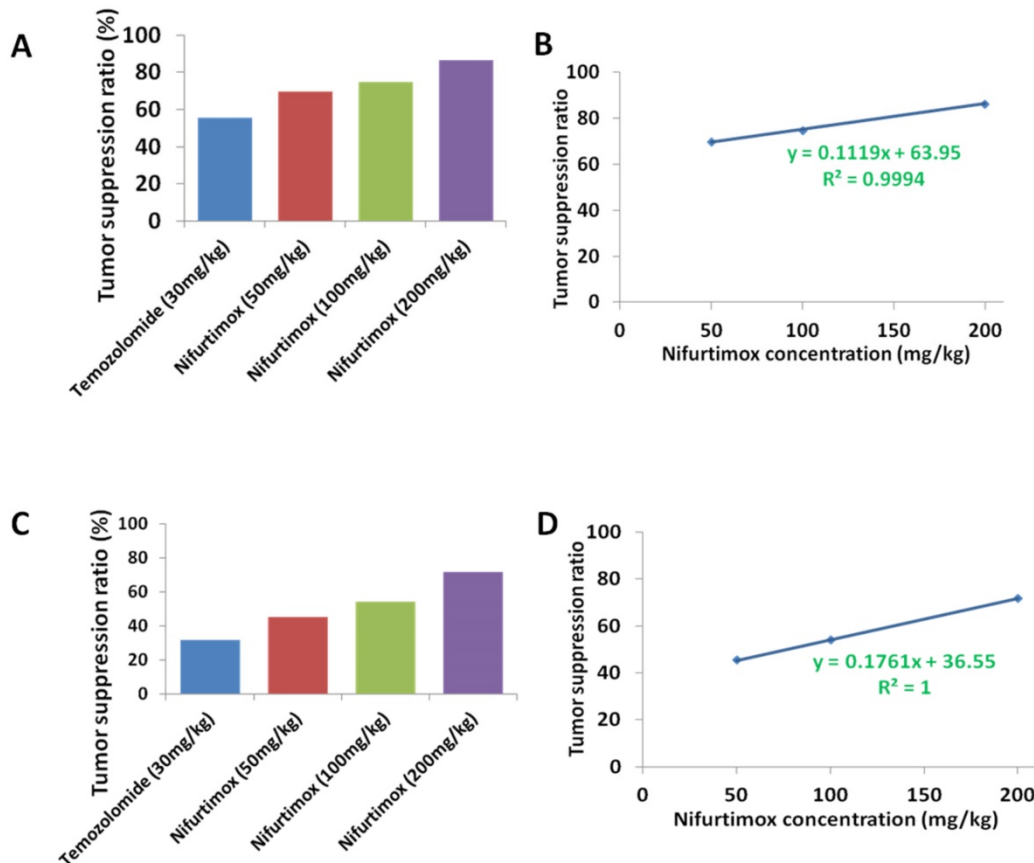

Figure 5. The tumor suppression ratio correlated with the dosage of the Nifurtimox. A and C) the tumor suppression ratio was calculated according to either the tumor-fluorescence intensity or the kidney weight with that of their control. B and D) The obtained tumor suppression ratio correlated perfectly with the dosage of Nifurtimox, R^2= 0.9994 or, R^2= 1.
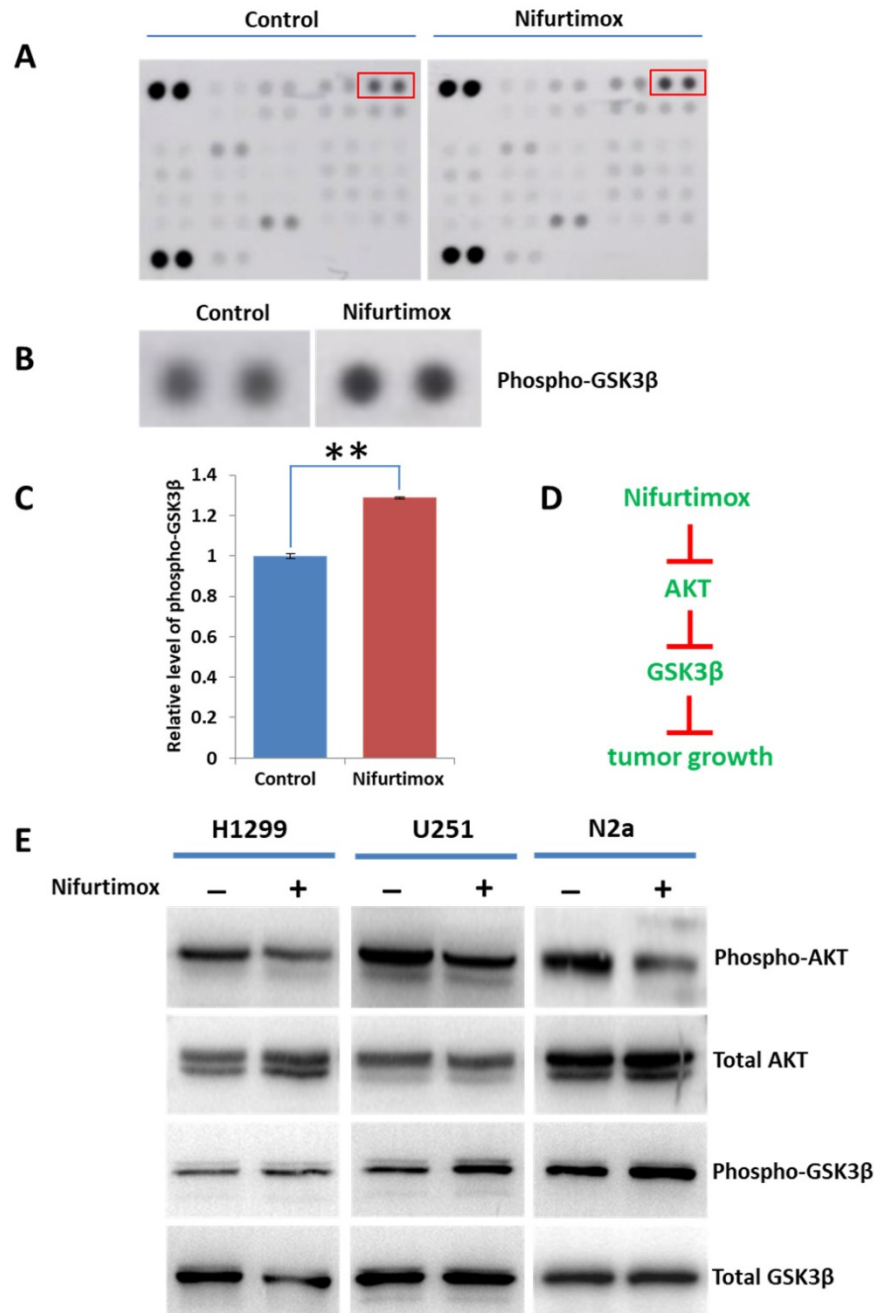
Figure 6. AKT-GSK3βsignaling is involved in tumor-suppression induced by nifurtimox. (A-C) Nifurtimox-treated and –untreated SH-SY5Y cells were assayed with Phospho-kinase array, the dot blot was quantified to show that the phosphorylation of GSK3β was significantly upregulated in nifurtimox-treated group. (D) Illustration showed the potential signaling cascade triggered by nifurtimox on the inhibition of tumor growth. (E) The phosphorylation level of Akt and GSK-3 β was inhibited by nifurtimox in different cell types e.g. H1299, U251 and N2a. ** p≤0.01 was labeled as compared with Control group.

Together, our study supported the notion that nifurtimox could suppress the neuroblastoma development efficiently while minimizing the worsening of the health condition to a great extent. Importantly, nifurtimox presented a stronger effect over temozolomide on inhibiting tumor progression and balancing the body weight, strongly suggested that nifurtimox could become a potential alternative drug in treating neuroblastoma.

Competing Interests

The authors have declared that no competing interest exists.

References

1. Park JR, Bagatell R, Cohn SL, Pearson AD, Villablanca JG, Berthold F, et al. Revisions to the International Neuroblastoma Response Criteria: A Consensus Statement From the National Cancer Institute Clinical Trials Planning Meeting. Journal of clinical oncology : official journal of the American Society of Clinical Oncology. 2017; 35: 2580-7.
2. Brodeur GM, Bagatell R. Mechanisms of neuroblastoma regression. Nature reviews Clinical oncology. 2014; 11: 704-13.

3.   Brodeur GM. Neuroblastoma: biological insights into a clinical enigma. Nature reviews Cancer. 2003; 3: 203-16.
4.   Maris JM, Hogarty MD, Bagatell R, Cohn SL. Neuroblastoma. Lancet (London, England). 2007; 369: 2106-20.
5.   Xu Y, Wang J, Peng Y, Zeng J. CT characteristics of primary retroperitoneal neoplasms in children. European journal of radiology. 2010; 75: 321-8.
6.   Wang Q, Diskin S, Rappaport E, Attiyeh E, Mosse Y, Shue D, et al. Integrative genomics identifies distinct molecular classes of neuroblastoma and shows that multiple genes are targeted by regional alterations in DNA copy number. Cancer research. 2006; 66: 6050-62.
7.   Brodeur GM, Maris JM, Yamashiro DJ, Hogarty MD, White PS. Biology and genetics of human neuroblastomas. Journal of pediatric hematology/oncology. 1997; 19: 93-101.
8.   Cabanillas Stanchi KM, Bruchelt G, Handgretinger R, Holzer U. Nifurtimox reduces N-Myc expression and aerobic glycolysis in neuroblastoma. Cancer biology & therapy. 2015; 16: 1353-63.
9.   Orbach D, Sarnacki S, Brisse HJ, Gauthier-Villars M, Jarreau PH, Tsatsaris V, et al. Neonatal cancer. The Lancet Oncology. 2013; 14: e609-20.
10. Dumba M, Jawad N, McHugh K. Neuroblastoma and nephroblastoma: a radiological review. Cancer imaging : the official publication of the International Cancer Imaging Society. 2015; 15: 5.
11. Le Loup G, Pialoux G, Lescure FX. Update in treatment of Chagas disease. Current opinion in infectious diseases. 2011; 24: 428-34.
12. Rassi A, Jr., Rassi A, Marin-Neto JA. Chagas disease. Lancet (London, England). 2010; 375: 1388-402.
13. Bern C. Antitrypanosomal therapy for chronic Chagas' disease. The New England journal of medicine. 2011; 364: 2527-34.
14. Solari A, Ortiz S, Soto A, Arancibia C, Campillay R, Contreras M, et al. Treatment of Trypanosoma cruzi-infected children with nifurtimox: a 3 year follow-up by PCR. The Journal of antimicrobial chemotherapy. 2001; 48: 515-9.
15. Du M, Zhang L, Scorsone KA, Woodfield SE, Zage PE. Nifurtimox Is Effective Against Neural Tumor Cells and Is Synergistic with Buthionine Sulfoximine. Scientific reports. 2016; 6: 27458.
16. Li Q, Lin Q, Kim H, Yun Z. The anti-protozoan drug nifurtimox preferentially inhibits clonogenic tumor cells under hypoxic conditions. American journal of cancer research. 2017; 7: 1084-95.
17. Saulnier Sholler GL, Kalkunte S, Greenlaw C, McCarten K, Forman E. Antitumor activity of nifurtimox observed in a patient with neuroblastoma. Journal of pediatric hematology/oncology. 2006; 28: 693-5.
18. Mesu V, Kalonji WM, Bardonneau C, Mordt OV, Blesson S, Simon F, et al. Oral fexinidazole for late-stage African Trypanosoma brucei gambiense trypanosomiasis: a pivotal multicentre, randomised, non-inferiority trial. Lancet (London, England). 2018; 391: 144-54.
19. Saulnier Sholler GL, Brard L, Straub JA, Dorf L, Illeyne S, Koto K, et al. Nifurtimox induces apoptosis of neuroblastoma cells in vitro and in vivo. Journal of pediatric hematology/oncology. 2009; 31: 187-93.
20. Docampo R, Mason RP, Mottley C, Muniz RP. Generation of free radicals induced by nifurtimox in mammalian tissues. The Journal of biological chemistry. 1981; 256: 10930-3.
21. Friedman HS, Kerby T, Calvert H. Temozolomide and treatment of malignant glioma. Clinical cancer research : an official journal of the American Association for Cancer Research. 2000; 6: 2585-97.
22. Ostermann S, Csajka C, Buclin T, Leyvraz S, Lejeune F, Decosterd LA, et al. Plasma and cerebrospinal fluid population pharmacokinetics of temozolomide in malignant glioma patients. Clinical cancer research : an official journal of the American Association for Cancer Research. 2004; 10: 3728-36.
23. Castel V, Segura V, Berlanga P. Emerging drugs for neuroblastoma. Expert opinion on emerging drugs. 2013; 18: 155-71.
24. Watson CP, Dogruel M, Mihoreanu L, Begley DJ, Weksler BB, Couraud PO, et al. The transport of nifurtimox, an anti-trypanosomal drug, in an in vitro model of the human blood-brain barrier: evidence for involvement of breast cancer resistance protein. Brain research. 2012; 1436: 111-21.
25. Jeganathan S, Sanderson L, Dogruel M, Rodgers J, Croft S, Thomas SA. The distribution of nifurtimox across the healthy and trypanosome-infected murine blood-brain and blood-cerebrospinal fluid barriers. The Journal of pharmacology and experimental therapeutics. 2011; 336: 506-15.
26. Stevens MF, Hickman JA, Langdon SP, Chubb D, Vickers L, Stone R, et al. Antitumor activity and pharmacokinetics in mice of 8-carbamoyl-3-methyl-imidazo[5,1-d]-1,2,3,5-tetrazin-4(3H)-one (CCRG 81045; M & B 39831), a novel drug with potential as an alternative to dacarbazine. Cancer research. 1987; 47: 5846-52.
27. Friedman HS, Dolan ME, Pegg AE, Marcelli S, Keir S, Catino JJ, et al. Activity of temozolomide in the treatment of central nervous system tumor xenografts. Cancer research. 1995; 55: 2853-7.
28. Plowman J, Waud WR, Koutsoukos AD, Rubinstein LV, Moore TD, Grever MR. Preclinical antitumor activity of temozolomide in mice: efficacy against human brain tumor xenografts and synergism with 1,3-bis(2-chloroethyl)-1-nitrosourea. Cancer research. 1994; 54: 3793-9.
29. Horgan CM, Tisdale MJ. Antitumour imidazotetrazines--IV. An investigation into the mechanism of antitumour activity of a novel and potent antitumour agent, mitozolomide (CCRG 81010, M & B 39565; NSC 353451). Biochemical pharmacology. 1984; 33: 2185-92.
30. Denny BJ, Wheelhouse RT, Stevens MF, Tsang LL, Slack JA. NMR and molecular modeling investigation of the mechanism of activation of the antitumor drug temozolomide and its interaction with DNA. Biochemistry. 1994; 33: 9045-51.
31. Doles JD, Hogan KA, O'Connor J, Wahner Hendrickson AE, Huston O, Jatoi A. Does the Poly (ADP-Ribose) Polymerase Inhibitor Veliparib Merit Further Study for Cancer-Associated Weight Loss? Observations and Conclusions from 60 Prospectively Treated Patients. Journal of palliative medicine. 2018.
32. de van der Schueren MAE, Laviano A, Blanchard H, Jourdan M, Arends J, Baracos VE. Systematic review and meta-analysis of the evidence for oral nutritional intervention on nutritional and clinical outcomes during chemo(radio)therapy: current evidence and guidance for design of future trials. Annals of oncology : official journal of the European Society for Medical Oncology. 2018; 29: 1141-53.
33. Lau SKM, Gannavarapu BS, Carter K, Gao A, Ahn C, Meyer JJ, et al. Impact of Socioeconomic Status on Pretreatment Weight Loss and Survival in Non-Small-Cell Lung Cancer. Journal of oncology practice. 2018; 14: e211-e20.
34. Saulnier Sholler GL, Bergendahl GM, Brard L, Singh AP, Heath BW, Bingham PM, et al. A phase 1 study of nifurtimox in patients with relapsed/refractory neuroblastoma. Journal of pediatric hematology/oncology. 2011; 33: 25-30.
35. Jin Z, Cheng X, Feng H, Kuang J, Yang W, Peng C, et al. Apatinib Inhibits Angiogenesis Via Suppressing Akt/GSK3beta/ANG Signaling Pathway in Anaplastic Thyroid Cancer. Cellular physiology and biochemistry : international journal of experimental cellular physiology, biochemistry, and pharmacology. 2017; 44: 1471-84.
36. Zhao L, Miao HC, Li WJ, Sun Y, Huang SL, Li ZY, et al. LW-213 induces G2/M cell cycle arrest through AKT/GSK3beta/beta-catenin signaling pathway in human breast cancer cells. Molecular carcinogenesis. 2016; 55: 778-92.